Error Rate and Ergodic Capacity of RF-FSO System with Partial Relay Selection in the Presence of Pointing Errors

Milica I. Petkovic[a,*], Imran Shafique Ansari[b], Goran T. Djordjevic[c], Khalid A. Qaraqe[d]

[a] *University of Novi Sad, Faculty of Technical Sciences, Department of Power, Electronics and Communications Engineering, Trg Dositeja Obradovica 6, 21000 Novi Sad, Serbia*
[b] *School of Engineering, University of Glasgow, Glasgow G12 8QQ, United Kingdom*
[c] *University of Nis, Faculty of Electronic Engineering, Department of Telecommunications, A. Medvedeva 14, 18000 Nis, Serbia*
[d] *Electrical and Computer Engineering (ECEN) Department, Texas A&M University at Qatar (TAMUQ), Education City, Doha, Qatar*

Abstract

This paper presents an analysis of a multiple dual-hop relaying system, which is composed of km-class radio frequency (RF)-free-space optical (FSO) links. Partial relay selection based on outdated channel state information (CSI) is employed in order to select active relay for further transmission. Amplify-and-forward relaying protocol is utilized. The RF links are assumed to be subject to Rayleigh fading, and the FSO links are influenced by both Gamma-Gamma atmospheric turbulence and pointing errors. On the basis of our previously derived expression for cumulative distribution function of the equivalent signal-to-noise ratio of the whole system, we derive novel analytical expressions for the average bit-error rate (BER) and ergodic capacity that are presented in terms of the Meijer's G-function and extended generalized bivariate Meijer's G-function, respectively. The numerical results are confirmed by Monte Carlo simulations. Considering the effect of time-correlation between outdated CSI and actual CSI related to the RF channel at the time of transmission, the average BER and the ergodic capacity dependence on various system and channel parameters are

*Corresponding author
Email address: milica.petkovic@uns.ac.rs (Milica I. Petkovic)

observed and discussed. The results illustrate that the temporal correlation between outdated and actual CSI has strong effect on system performance, particularly on BER values, when FSO hop is influenced by favorable conditions.
Keywords: Bit error rate, ergodic capacity, free-space optical systems, partial relay selection, radio frequency systems.

---

1. Introduction

Radio frequency (RF) systems, which are very often used for backhaul networking, cannot support high data rates of great number of users and other requirements of the 5^{th} generation wireless networks [1]. Because of that, free-space (FSO) optical systems have been adopted as a complement or alternative to the radio frequency (RF) technology, especially in overcoming the connectivity hole between the main backbone system and last mile access network. The use of FSO systems provides a license-free and high data rates transmission [2, 3, 4, 5, 6, 7, 8]. The FSO links are valuable for enabling a large number of RF users to be multiplexed through a single FSO link. Ciaramella *et al.* [9] realized an FSO system between two buildings in Pisa, Italy, and reached the date rate of 1.28 Tb/s over a distance of 210 m. The recent experiment, carried out by German Aerospace Center (DLR), proved that data rate of 1.72 Tb/s can be achieved over an FSO link with length of 10.45 km [10]. These experimental demonstrations proved that FSO could be a promising technology for achieving high quality-of-services and high data rates in 5G networks.

The main reason for the intensity fluctuations of the received optical signal is atmospheric turbulence, which occurs as a result of the variations in atmospheric altitude, temperature, and pressure. The misalignment between the transmitter laser and the detector at the receiver (called pointing errors) is another cause of intensity fluctuations of the optical signal. Although received optical signal fluctuations can be mitigated by diversity techniques [11], and a number of techniques have been developed to ensure alignment between transmitter and receiver of FSO link [12], these two effects have attracted attention of many

researchers [13, 14, 15, 16]. The Gamma-Gamma distribution is widely adopted for modeling intensity fluctuations due to atmospheric turbulence [11, 17, 18, 19, 20], while the pointing errors are described by the model derived with an assumption that the total radial displacement at the receiver detector is subject to Rayleigh distribution [13, 14, 15, 16]. That means transmitter and receiver are aligned initially perfectly, but due to beam wandering and building sway, tracking is not perfect and random misalignment appears. This assumption is relevant for FSO links with km-class lengths.

The main challenge in the FSO link implementation is the obligatory presence of the line-of-sight (LOS) between FSO apertures. Since the realization of this LOS requirement is quite challenging in some scenarios (difficult terrains such as crowded urban streets and areas), the idea of utilizing relaying technology within FSO systems has been arised to accomplish coverage area extension. More precisely, the mixed (asymmetric) dual-hop amplify-and-forward (AF) RF-FSO relaying system, composed of RF and FSO links, was firstly introduced in [21]. In order to perform electrical-to-optical signal conversion at the relay, subcarrier intensity modulation (SIM) technique can be applied [11, 22]. In addition, the mixed RF-FSO systems enable multiple RF users to be multiplexed via a single FSO link [23]. Besides [21], the performance analysis of the asymmetric RF-FSO systems with employing fixed AF gain relay was investigated in [22, 23, 24, 25, 26, 27, 28, 29, 30, 31]. Contrary, the performance of the asymmetric RF-FSO systems with employing variable AF gain relay was presented in [31, 32, 33, 34, 35], while [36] considered decode-and-forward RF-FSO system. Additionally, the impact of the interference at relay on the overall system performance was investigated in [37, 38]. The multiuser RF-FSO system was analyzed in [39, 40, 41, 42]. In order to expand range and improve the performance limitations of FSO communications, triple-hop RF/FSO/RF communication system was proposed in [43, 44].

With aim to improve the system performance, implementation of multiple relays in RF systems were widely investigated in past literature [45, 46, 47, 48, 49, 50, 51, 52]. In order to avoid additional network delays and to achieve power

savings, the partial relay selection (PRS) was introduced in [47], considering the scenario when the active relay is chosen on the basis of single-hop instantaneous channel state information (CSI).

The idea of PRS procedure utilization in the asymmetric RF-FSO systems employing fixed AF relays was proposed in [53], wherein the first RF hops experience Rayleigh fading, and the second FSO hops are affected by the Gamma-Gamma atmospheric turbulence. In addition, the impact of the pointing errors on the same system was observed in [54], providing the novel expressions for the outage probability. In [55], the multiple relayed mixed RF-FSO system with PRS was analyzed, but the FSO link was influenced by Double Generalized Gamma atmospheric turbulence. Furthermore, performance analysis of the RF-FSO system with multiple relays was performed in [56, 57], taking into account hardware impairments.

The previous studies [54, 55] was concentrated on determining outage probability. However, besides outage probability, other performance metrics are also important. From both users' and designers' point of view, it is very important to know the probability that a bit transmitted over a channel will be wrongly detected, known as bit error rate. In addition, we are focused on determining the maximum data rate that could be supported by a channel when error probability can be downscaled under arbitrary low value. In this work, we extend the analysis from [54] to estimating of ergodic capacity and average bit error rate (BER). Although the system model is quite similar compared with the one presented in [54], analytical derivations are completely novel, and numerical results have not been previously reported. Novel analytical expressions for the average BER and the ergodic capacity are derived in terms of the Meijer's G-function and the extended generalized bivariate Meijer's G-function (EGBMGF), respectively. These expressions are utilized for examining some interesting effects of FSO and RF channels parameters on overall system performance. The analysis is carried out in the case when RF intermediate-frequency signal is amplified and modulated in optical carrier.

The remainder of the paper is organized in the following way. Channel

and system models are described in Section 2. Section 3 gives the average BER and the ergodic capacity analysis. Numerical results and simulations with corresponding comments are given in Section 4, while Section 5 concludes the paper.

2. System and channel model

The paper presents the analysis of the RF-FSO relaying system, assuming that the signal transmission from source to the active relay is performed in frequency range from 900 MHz to 2.4 GHz. Asymmetric AF dual-hop RF-FSO system, presented in Fig. 1, consists of source S, destination D, and $M \geq 1$ relays, assuming there is no direct link between S and D nodes. Based on the local feedback sent from the relays, the source node S monitors the conditions of the first RF hops, and selects the active relay for further transmission via FSO channel. Active relay is selected as the best one on the basis of estimated CSIs of the RF hops. Since time-varying nature of the RF hops is usual in practical scenarios, and due to feedback delay, the estimated CSI is not the same as actual one at the time of signal transmission. Because of that reason, following analysis considers the estimated CSI as outdated and time-correlated with the actual CSI of the RF hop. In addition, the selected active relay is not maybe available. In that case, the source chooses the next best relay, etc., and the PRS procedure is performed via the lth worst (or $(M-l)$th best) relay $R_{(l)}$ [50].

After the active relay selection, signal is transmitted over the selected RF hop. The electrical signal at the lth relay is defined as

$$r_{R(l)} = h_{SR(l)} r + n_{SR}, \tag{1}$$

where r represents a complex-valued baseband representation of the RF signal sent from the source node S with an average power P_s, $h_{SR(l)}$ is the fading amplitude over the $S-R_{(l)}$ hop with $\mathrm{E}\left[h_{SR(l)}^2\right] = 1$, ($\mathrm{E}[\cdot]$ denotes mathematical expectation), and n_{SR} denotes an additive white Gaussian noise with zero mean and variance σ_{SR}^2.

Based on (1), the instantaneous signal-to-noise ratio (SNR) of the first RF hop is defined as

$$\gamma_{1(l)} = \frac{h_{SR(l)}^2 P_s}{\sigma_{SR}^2} = h_{SR(l)}^2 \mu_1, \tag{2}$$

where μ_1 is the average SNR defined as $\mu_1 = P_s/\sigma_{SR}^2$.

The signal $r_{R(l)}$ is amplified by the fixed gain G at the relay. The amplification is performed based on long-term statistic of the first RF hop. In this case, the relay gain G is determined as [51]

$$G^2 = \frac{1}{\mathrm{E}\left[h_{SR(l)}^2\right] P_s + \sigma_{SR}^2} = \frac{1}{\sigma_{SR}^2 \left(\mathrm{E}\left[\gamma_{1(l)}\right] + 1\right)} = \frac{1}{\sigma_{SR}^2 \Re}, \tag{3}$$

where $\Re = \mathrm{E}\left[\gamma_{1(l)}\right] + 1$.

The amplified signal modulates an optical source (laser) intensity. The non-negativity requirement is ensured by adding dc bias. The optical signal at the relay output is given by

$$r_{opt} = P_t \left(1 + G m r_{R(l)}\right), \tag{4}$$

where P_t denotes transmitted optical power and m is the modulation index ($m = 1$). Signal is transmitted via free space and collected by the receiving telescope.

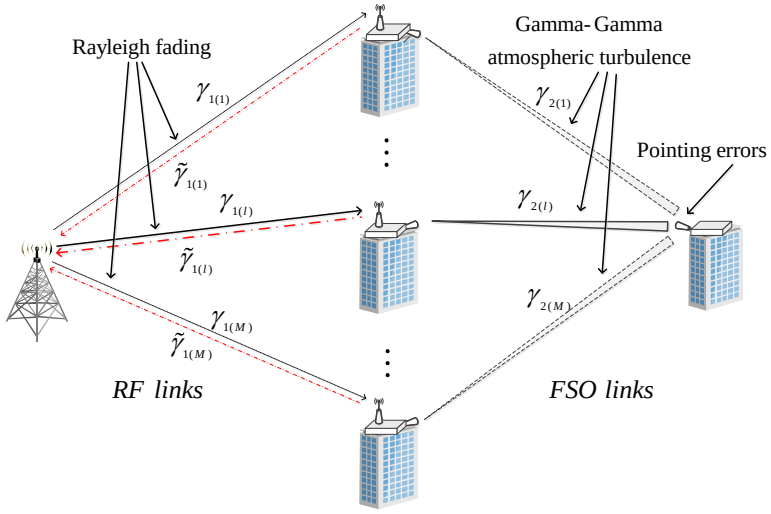

Figure 1: Mixed RF-FSO system with PRS

Direct detection is performed and dc bias is removed. PIN photodetector is employed to perform an optical-to-electrical signal conversion. The electrical signal at the node D is given by

$$\begin{aligned} r_{D(l)} &= I_{R(l)D}\eta P_t G r_{R(l)} + n_{RD} \\ &= I_{R(l)D}\eta P_t G h_{SR(l)} r + I_{R(l)D}\eta P_t G n_{SR} + n_{RD}, \end{aligned} \tag{5}$$

where $I_{R(l)D}$ represents the received optical signal intensity, and n_{RD} represents the thermal noise modeled by the Gaussian distribution with zero mean and variance σ_{RD}^2. An optical-to-electrical conversion coefficient is denoted by η.

Based on (3) and (5), the overall SNR at the destination is [54]

$$\gamma_{eq} = \frac{I_{R(l)D}^2 \eta^2 P_t^2 G^2 h_{SR(l)}^2 P_s}{I_{R(l)D}^2 \eta^2 P_t^2 G^2 \sigma_{SR}^2 + \sigma_{RD}^2} = \frac{\gamma_{1(l)}\gamma_{2(l)}}{\gamma_{2(l)} + \Re}, \tag{6}$$

where $\gamma_{2(l)}$ represents the instantaneous SNR over FSO link, given by

$$\gamma_{2(l)} = \frac{I_{R(l)D}^2 \eta^2 P_t^2}{\sigma_{RD}^2}. \tag{7}$$

The electrical SNR over FSO link is defined as
$\mu_2 = \eta^2 P_t^2 \mathrm{E}^2\left[I_{R(l)D}\right]/\sigma_{RD}^2$.

2.1. RF channel model

The source monitors the conditions of the first RF hops by local feedbacks sent from relays. The active relay is selected based on the estimated CSIs of all RF hops. The estimated CSIs are assumed to be outdated and time-correlated with the actual corresponding CSIs of the RF hops. Furthermore, the fact that the best selected relay is not necessarily available for further transmission is taken into consideration.

The RF hops are subject to Rayleigh fading. The probability density function (PDF) of the instantaneous SNR per RF hop between the source and the lth relay is derived in detail in [50, 53, 54], and is given by

$$f_{\gamma_{1(l)}}(x) = l\binom{M}{l}\sum_{i=0}^{l-1}\binom{l-1}{i}\frac{(-1)^i}{\mu_1((M-l+i)(1-\rho)+1)} e^{-\frac{(M-l+i+1)x}{((M-l+i)(1-\rho)+1)\mu_1}}, \tag{8}$$

where ρ represents correlation coefficient between the instantaneous SNR over RF hop at the time of transmission ($\gamma_{1(l)}$) and its outdated estimated version ($\tilde{\gamma}_{1(l)}$), which is used for relay selection.

The cumulative distribution function (CDF) of $\gamma_{1(l)}$ is

$$F_{\gamma_{1(l)}}(x) = 1 - l\binom{M}{l}\sum_{i=0}^{l-1}\binom{l-1}{i}\frac{(-1)^i}{(M-l+i+1)}e^{-\frac{(M-l+i+1)x}{((M-l+i)(1-\rho)+1)\mu_1}}. \quad (9)$$

The constant $\Re$ is found by (3) and (8) as [51, (6)]

$$\Re = 1 + l\binom{M}{l}\sum_{i=0}^{l-1}\binom{l-1}{i}\frac{(-1)^i\left((M-l+i)(1-\rho)+1\right)\mu_1}{(M-l+i+1)^2}. \quad (10)$$

2.2. FSO channel model

The considered system assumes that the intensity fluctuations of optical signal at the destination originate from the Gamma-Gamma atmospheric turbulence and pointing errors. The PDF of $I_{R(l)D}$ is [14, (12)]

$$f_{I_{R(l)D}}(I_{R(l)D}) = \frac{\psi^2\alpha\beta}{A_0\Gamma(\alpha)\Gamma(\beta)}G_{1,3}^{3,0}\left(\frac{\alpha\beta}{A_0}I_{R(l)D}\,\middle|\,{}^{\psi^2}_{\psi^2-1,\,\alpha-1,\,\beta-1}\right), \quad (11)$$

where $G_{p,q}^{m,n}(\cdot)$ is Meijer's G-function [58, (9.301)]. Note that received signal variations due to scintillation and pointing errors are taken into account by (11). The deterministic path loss due to scattering and diffraction [11, 12] can be straightforwardly included. The path loss is relevant in the case when results should be presented in terms of the radiated optical power. The parameters α and β are used to define an effective numbers of the scattering environment small-scale and large-scale cells, respectively, which are, with the assumption of the plane wave propagation and zero inner scale, defined as

$$\begin{aligned}\alpha &= \left(\exp\left[0.49\chi_R^2\Big/\left(1+1.11\chi_R^{12/5}\right)^{7/6}\right]-1\right)^{-1},\\ \beta &= \left(\exp\left[0.51\chi_R^2\Big/\left(1+0.69\chi_R^{12/5}\right)^{5/6}\right]-1\right)^{-1}.\end{aligned} \quad (12)$$

The Rytov variance is defined as $\chi_R^2 = 1.23C_n^2\iota^{7/6}d^{11/6}$, $\iota = 2\pi/\lambda$ represents the wave number with the wavelength λ, and d is the FSO link length. The refractive index structure parameter is denoted by C_n^2, varying in the range from

Table 1: Constants and system and channels parameters (unless otherwise is stated)

name	symbol	value
FSO link distance	d	2000 m
Refractive index structure parameter	C_n^2	6×10^{-15} m$^{-2/3}$ in weak turbulence
Refractive index structure parameter	C_n^2	2×10^{-14} m$^{-2/3}$ in moderate turbulence
Refractive index structure parameter	C_n^2	5×10^{-14} m$^{-2/3}$ in strong turbulence
Optical wavelength	λ	1.55 μm
Radius of a circular detector aperture	a	5 cm
Optical beam radius at the waist	a_0	5 cm
Pointing error (jitter) standard deviation	σ_s	5 cm
Number of relays	M	2
Order of selected relay	l	2

10^{-17} to 10^{-13} m$^{-2/3}$ for weak to strong turbulence. The parameter relating to the pointing errors, ψ, is defined as

$$\psi = \frac{a_{d_{eq}}}{2\sigma_s}, \tag{13}$$

where $a_{d_{eq}}$ is the equivalent beam radius at the receiver and σ_s represents the pointing error (jitter) standard deviation at the receiver. The parameter $a_{d_{eq}}$ is dependent on the beam radius at the distance d, a_d, as $a_{d_{eq}}^2 = a_d^2\sqrt{\pi}\mathrm{erf}(v)\big/(2v\exp(-v^2))$, with $v = \sqrt{\pi}a\big/(\sqrt{2}a_d)$ and the parameter a being the radius of a circular detector aperture. The parameter A_0 is defined as $A_0 = [\mathrm{erf}\,(v)]^2$, where $\mathrm{erf}\,(\cdot)$ is the error function [58, (8.250.1)].

The parameter a_d is related to the optical beam radius at the waist, a_0, and to the radius of curvature, F_0, as $a_d = a_0\Big((\Theta_o + \Lambda_o)(1 + 1.63\chi_R^{12/5}\Lambda_1)\Big)^{1/2}$, where $\Theta_o = 1 - d/F_0$, $\Lambda_o = 2d\big/(\iota a_0^2)$, and $\Lambda_1 = \Lambda_o\big/(\Theta_o^2 + \Lambda_o^2)$ [16]. As it has been mentioned, a standard deviation of pointing errors appears in (13). By varying this parameter, it is possible to model situation when the alignment between transmitter and receiver is almost perfect. On the other hand, it is also possible to increase standard deviation of pointing errors and describe correctly

the situation when tracking is not so precise.

Based on (11), the electrical SNR is found as $\mu_2 = \eta^2 P_t^2 \kappa^2 A_0^2 / \sigma_{RD}^2$, with $\kappa = \psi^2/(\psi^2+1)$. After some mathematical manipulations and utilizing (7) and (11), the PDF of $\gamma_{2(l)}$ is derived as [33]

$$f_{\gamma_{2(l)}}(\gamma_2) = \frac{\psi^2}{2\Gamma(\alpha)\Gamma(\beta)\gamma_2} G_{1,3}^{3,0}\left(\alpha\beta\kappa\sqrt{\frac{\gamma_2}{\mu_2}} \,\middle|\, \begin{matrix} \psi^2+1 \\ \psi^2,\, \alpha,\, \beta \end{matrix}\right). \tag{14}$$

System and channels parameters values, unless otherwise is stated in Numerical results section, are presented in Table I.

3. System performance analysis

This section presents the analysis of the system described in Section 2 with the aim of deriving analytical expressions for average BER and ergodic capacity. Derivations of average BER and ergodic capacity are based on knowing CDF of the equivalent SNR. This CDF is defined as

$$\begin{aligned} F_{eq}(\gamma_{th}) &= \Pr\left(\frac{\gamma_{2(l)}\gamma_{1(l)}}{\gamma_{2(l)} + \Re} < \gamma_{th}\right) \\ &= \int_0^\infty \Pr\left(\gamma_{1(l)} < \gamma_{th} + \frac{\gamma_{th}\Re}{\gamma_{2(l)}}\right) f_{\gamma_{2(l)}}\left(\gamma_{2(l)}\right) d\gamma_{2(l)} \\ &= \int_0^\infty F_{\gamma_{1(l)}}\left(\gamma_{th} + \frac{\gamma_{th}\Re}{x}\right) f_{\gamma_{2(l)}}(x)\, dx, \end{aligned} \tag{15}$$

where $\Pr(\cdot)$ denotes the probability. Substituting (9) and (14) into (15), after mathematical derivation presented in detail in [54], the final expression for CDF is derived as [54, (17.28)]

$$\begin{aligned} F_{eq}(\gamma_{th}) = 1 - l\binom{M}{l} \sum_{i=0}^{l-1} \binom{l-1}{i} \frac{(-1)^i}{(M-l+i+1)} e^{-\frac{(M-l+i+1)\gamma_{th}}{((M-l+i)(1-\rho)+1)\mu_1}} \\ \times \frac{2^{\alpha+\beta-3}\psi^2}{\pi\Gamma(\alpha)\Gamma(\beta)} G_{1,6}^{6,0}\left(\frac{\alpha^2\beta^2\kappa^2(M-l+i+1)\gamma_{th}\Re}{16\mu_2\left((M-l+i)(1-\rho)+1\right)\mu_1} \,\middle|\, \begin{matrix} \frac{\psi^2+2}{2} \\ \chi_1 \end{matrix}\right), \end{aligned} \tag{16}$$

where

$$\chi_1 = \frac{\psi^2}{2}, \quad \frac{\alpha}{2}, \quad \frac{\alpha+1}{2}, \quad \frac{\beta}{2}, \quad \frac{\beta+1}{2}, \quad 0. \tag{17}$$

If it is assumed that the pointing errors are small and negligible, it holds that the intensity fluctuations result only from atmospheric turbulence. In that case, the CDF is derived by taking the limit of (16) by using [61, (07.34.25.0007.01), (07.34.25.0006.01), and (06.05.16.0002.01))] and utilizing $\lim_{\xi\to\infty}\left(1+2/\xi^2\right)=1$ and $\lim_{\xi\to\infty}\kappa^2=\lim_{\xi\to\infty}\left(1+1/\xi^2\right)^2=1$. Obtained expression for the CDF (i.e., outage probability) is reported in [53, (15)].

3.1. Average BER

In the following analysis, the average BER expressions are derived in the case when two modulation formats are applied. More precisely, binary phase-shift keying (BPSK) or differential BPSK (DBPSK) [62] is applied over RF link and SIM-BPSK or SIM-DBPSK [11] is applied over FSO link. Following [23, 24, 63], the average BER of the system under investigation can be found as

$$P_b=\frac{q^p}{2\Gamma(p)}\int_0^\infty e^{-q\gamma}\gamma^{p-1}F_{eq}\left(\gamma\right)d\gamma, \tag{18}$$

where $F_{eq}\left(\gamma\right)$ is the derived CDF given by (16), and the parameters p and q are $(p,q)=(0.5,1)$ for BPSK and SIM-BPSK; $(p,q)=(1,1)$ for DBPSK and SIM-DBPSK.

Substituting (16) into (18), the average BER is obtained as

$$\begin{aligned}P_b=&\frac{q^p}{2\Gamma(p)}\int_0^\infty e^{-q\gamma}\gamma^{p-1}\left\{1-l\binom{M}{l}\sum_{i=0}^{l-1}\binom{l-1}{i}\frac{(-1)^i}{(M-l+i+1)}\right.\\&\times e^{-\frac{(M-l+i+1)\gamma}{((M-l+i)(1-\rho)+1)\mu_1}}\frac{2^{\alpha+\beta-3}\psi^2}{\pi\Gamma(\alpha)\Gamma(\beta)}\\&\left.\times G_{1,6}^{6,0}\left(\frac{\alpha^2\beta^2\kappa^2(M-l+i+1)\gamma_{th}\Re}{16\mu_2\left((M-l+i)(1-\rho)+1\right)\mu_1}\,\middle|\,\begin{matrix}\frac{\psi^2+2}{2}\\ \chi_1\end{matrix}\right)\right\}d\gamma\\&=\Im_1-\Im_2.\end{aligned} \tag{19}$$

The first integral in (19) is defined and solved using [58, (3.351.3)] as

$$\Im_1=\frac{q^p}{2\Gamma(p)}\int_0^\infty e^{-q\gamma}\gamma^{p-1}d\gamma=\frac{1}{2}. \tag{20}$$

After transforming the exponential function into Meijer's G-function by utilizing [61, (01.03.26.0004.01)], the integral $\Im_2$ is expressed as

$$\begin{aligned}\Im_2 = &\frac{q^p}{2\Gamma(p)} l \binom{M}{l} \sum_{i=0}^{l-1} \binom{l-1}{i} \frac{(-1)^i}{(M-l+i+1)} \frac{2^{\alpha+\beta-3}\psi^2}{\pi\Gamma(\alpha)\Gamma(\beta)} \\ &\times \int_0^\infty \gamma^{p-1} G_{0,1}^{1,0}\left(\left(q + \frac{(M-l+i+1)}{((M-l+i)(1-\rho)+1)\,\mu_1}\right)\gamma \,\middle|\, \begin{matrix} - \\ 0 \end{matrix}\right) \\ &\times G_{1,6}^{6,0}\left(\frac{\alpha^2\beta^2\kappa^2(M-l+i+1)\Re\gamma}{16\mu_2\left((M-l+i)(1-\rho)+1\right)\mu_1} \,\middle|\, \begin{matrix} \frac{\psi^2+2}{2} \\ \chi_1 \end{matrix}\right) d\gamma. \end{aligned} \tag{21}$$

After using [61, (07.34.21.0013.01)], the integral in (21) is obtained as

$$\begin{aligned}\Im_2 = &\frac{2^{\alpha+\beta-4}\psi^2}{\pi\Gamma(\alpha)\Gamma(\beta)\Gamma(p)} l \binom{M}{l} \sum_{i=0}^{l-1} \binom{l-1}{i} \\ &\times \frac{(-1)^i}{(M-l+i+1)} \left(1 + \frac{(M-l+i+1)}{((M-l+i)(1-\rho)+1)\,q\mu_1}\right)^{-p} \\ &\times G_{2,6}^{6,1}\left(\frac{\alpha^2\beta^2\kappa^2\Re}{16\mu_2\left(1+\frac{q\mu_1((M-l+i)(1-\rho)+1)}{(M-l+i+1)}\right)} \,\middle|\, \begin{matrix} 1-p, \frac{\psi^2+2}{2} \\ \chi_1 \end{matrix}\right). \end{aligned} \tag{22}$$

Substituting (20) and (22) into (19), the final average BER expression is obtained as

$$\begin{aligned}P_b = &\frac{1}{2} - \frac{2^{\alpha+\beta-4}\psi^2}{\pi\Gamma(\alpha)\Gamma(\beta)\Gamma(p)} l \binom{M}{l} \sum_{i=0}^{l-1} \binom{l-1}{i} \\ &\times \frac{(-1)^i}{(M-l+i+1)} \left(1 + \frac{(M-l+i+1)}{((M-l+i)(1-\rho)+1)\,q\mu_1}\right)^{-p} \\ &\times G_{2,6}^{6,1}\left(\frac{\alpha^2\beta^2\kappa^2\Re}{16\mu_2\left(1+\frac{q\mu_1((M-l+i)(1-\rho)+1)}{(M-l+i+1)}\right)} \,\middle|\, \begin{matrix} 1-p, \frac{\psi^2+2}{2} \\ \chi_1 \end{matrix}\right). \end{aligned} \tag{23}$$

Under the assumption that the pointing errors are neglected, and the intensity fluctuations are caused only from atmospheric turbulence, the average BER can be obtained by taking the limit of (23), which presents the average BER expression already reported in [53, (26)].

3.2. Ergodic capacity

The assumption is that interleaving is applied at the input of mixed RF-FSO link. This interleaving ensures the FSO channel scintillation remains constant

over a frame of symbols and changes for neighboring blocks based on Gamma-Gamma PDF. Similarly, RF channel fading is constant over a frame and changes from one to the next frame based on Rayleigh PDF. In addition, a Gaussian codebook is at the channel input. This codebook is long enough to enable scintillation/fading to be properly described by their PDFs. The ergodic capacity of this composite channel tells us that the maximum information transmission rate is when error probability can be arbitrary low. This is theoretical limit and could be achieved only under previously mentioned conditions. This ergodic capacity should be understood as a benchmark for a given composite RF-FSO channel. Some details related with designing of interleaver depth, which will be sufficient to ensure statistical independence of scintillation/fading from frame to frame, are given in Subsection II.*C*.

For the system under investigation, the ergodic channel capacity, which is determined as $\hat{C}$=E $[\log_2 (1 + e/ (2\,\pi)\ \gamma)]$ in bits/s/Hz [64, 65] (and see references therein), can be derived as

$$\hat{C} = B \int_0^{\infty} \log_2 (1 + e/ (2\,\pi)\ \gamma)\, f_{\gamma_{eq}} (\gamma)\, d\gamma, \tag{24}$$

where a channel bandwidth is denoted by B, and $f_{\gamma_{eq}} (\cdot)$ represents the PDF of overall SNR at the destination. Using integration by parts, the ergodic channel capacity in (24) can be presented in terms of the complementary CDF (CCDF) as [66]

$$\hat{C} = B \frac{1}{\ln 2} \int_0^{\infty} \frac{e}{2\pi} \frac{F^c_{\gamma_{eq}} (\gamma)}{1 + e/ (2\,\pi)\ \gamma} d\gamma, \tag{25}$$

where $F^c_{\gamma_{eq}} (\gamma)$ is the CCDF of overall SNR defined as $F^c_{\gamma_{eq}} (\gamma) = 1 - F_{\gamma_{eq}} (\gamma)$ ($F_{\gamma_{eq}}$ is the CDF in (16)). After substituting (16) into (25), and after applying [61, (01.02.26.0007.01)]

$$(1 + e/ (2\,\pi)\ \gamma)^{-1} = \frac{1}{\Gamma (1)} G^{1,1}_{1,1}(e/ (2\,\pi)\ \gamma \,|\, {}^{0}_{0}), \tag{26}$$

and [61, (01.03.26.0004.01)]

$$e^{-\frac{(M-l+i+1)\gamma}{((M-l+i)(1-\rho)+1)\mu_1}} = G^{1,0}_{0,1}\left(\frac{(M-l+i+1)\gamma}{((M-l+i)(1-\rho)+1)\,\mu_1} \,\middle|\, {}^{-}_{0} \right), \tag{27}$$

the ergodic capacity in (25) is expressed as

$$\begin{aligned}\hat{C} = B\frac{2^{\alpha+\beta-3}\psi^2}{\ln 2\pi\Gamma(\alpha)\Gamma(\beta)}l\binom{M}{l}\sum_{i=0}^{l-1}\binom{l-1}{i}\frac{(-1)^i e}{(M-l+i+1)2\pi}\\ \times\int_0^\infty G_{1,1}^{1,1}\Big(\frac{e}{2\,\pi}\,\gamma\,\Big|\,{}^{0}_{0}\Big)G_{0,1}^{1,0}\Big(\frac{(M-l+i+1)\gamma}{((M-l+i)(1-\rho)+1)\,\mu_1}\,\Big|\,{}^{-}_{0}\Big)\\ \times G_{1,6}^{6,0}\Big(\frac{\alpha^2\beta^2\kappa^2(M-l+i+1)\gamma\Re}{16\mu_2\,((M-l+i)(1-\rho)+1)\,\mu_1}\,\Big|\,{}^{\frac{\psi^2+2}{2}}_{\chi_1}\Big)d\gamma.\end{aligned} \tag{28}$$

The integral in (28) can be solved by using [67, (12)]. The final ergodic capacity is obtained in terms of the EGBMGF [63] as

$$\begin{aligned}\hat{C} = B\frac{2^{\alpha+\beta-3}\psi^2}{\ln 4\pi^2\Gamma(\alpha)\Gamma(\beta)}l\binom{M}{l}\sum_{i=0}^{l-1}\binom{l-1}{i}\frac{(-1)^i e((M-l+i)(1-\rho)+1)\mu_1}{(M-l+i+1)^2}\\ \times G_{1,0:1,1:6,0}^{1,0:1,1:6,0}\left(\begin{array}{c|c|c}1 & 0 & \frac{\psi^2+2}{2}\\ - & 0 & \chi_1\end{array}\,\Big|\,\mathrm{A},\mathrm{B}\right),\end{aligned} \tag{29}$$

where $\mathrm{A} = \frac{((M-l+i)(1-\rho)+1)e\mu_1}{(M-l+i+1)2\,\pi}$ and $\mathrm{B} = \frac{\alpha^2\beta^2\kappa^2\Re}{16\mu_2}$.

4. Numerical results and simulations

Based on the derived expressions for the average BER and the ergodic capacity, we obtain numerical results, which are validated via Monte Carlo simulations. The expression in (29) is calculated by using the MATHEMATICA implementation of the EGBMGF given in [63, Table II]. Atmospheric turbulence strength is determined by the refractive index structure parameter for different conditions: $C_n^2 = 6 \times 10^{-15}$ m$^{-2/3}$ for weak, $C_n^2 = 2 \times 10^{-14}$ m$^{-2/3}$ for moderate, and $C_n^2 = 5 \times 10^{-14}$ m$^{-2/3}$ for strong turbulence conditions.

Fig. 2 presents the average BER dependence on the average SNR over RF hop in different atmospheric turbulence conditions. Two situations are identified: in the first case μ_2 has a constant value of 30 dB in the whole range of μ_1, while in the second case μ_2 is equal to μ_1 in the whole range of observation. As

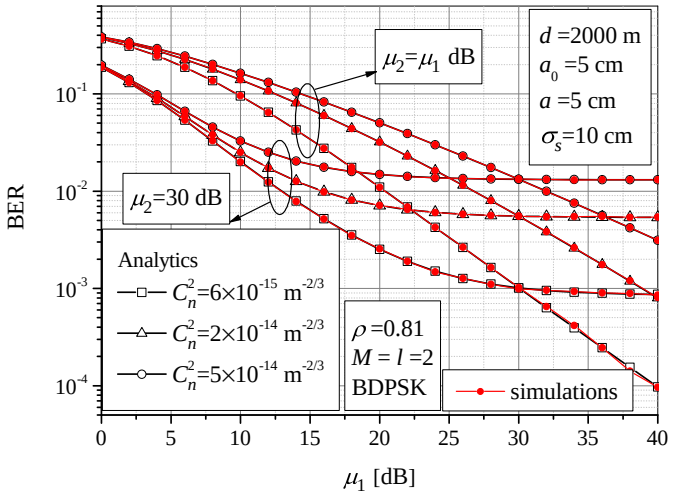

Figure 2: Average BER vs. μ_1 in various atmospheric turbulence conditions

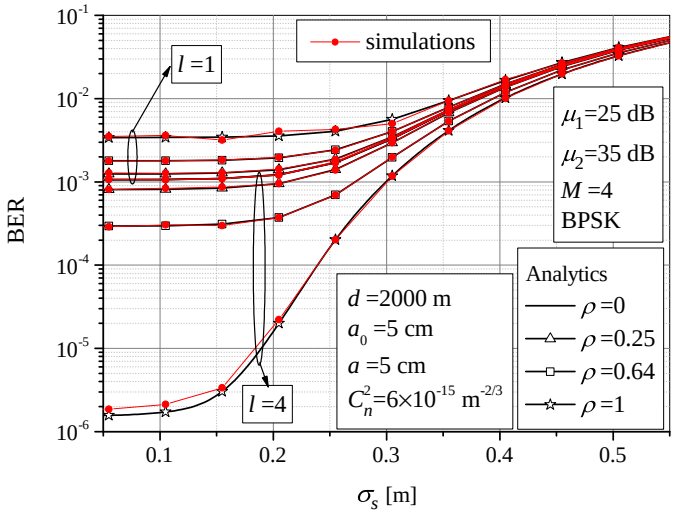

Figure 3: Average BER vs. σ_s for different values of correlation coefficient

it is expected, system performance is better when the value of C_n^2 is lower, corresponding to better conditions for the optical signal transmission. When μ_2 takes a constant value, the average BER floor occurs, and further increasing the signal power does not improve the system performance. This average BER floor occurs in the range of lower values of μ_1 when the FSO hop is under the

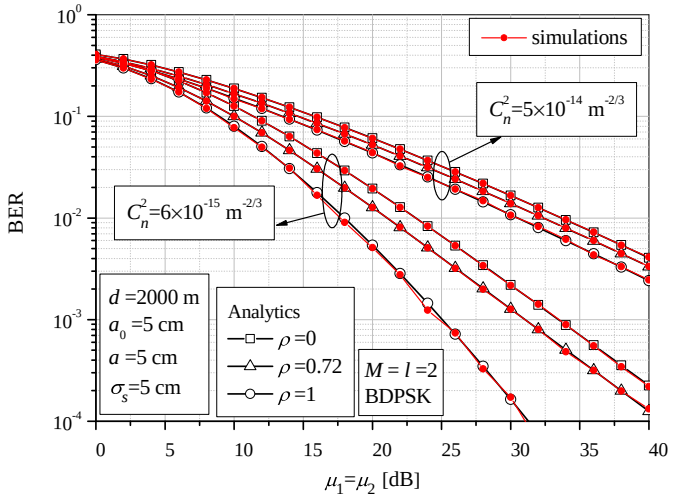

Figure 4: Average BER vs. $\mu_1 = \mu_2$ in various atmospheric turbulence conditions for different values of correlation coefficient

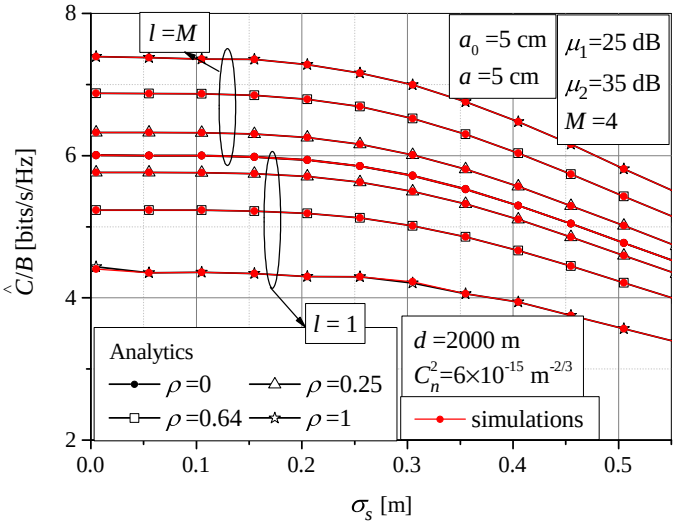

Figure 5: Ergodic capacity vs. σ_s for different values of correlation coefficient

influence of stronger atmospheric turbulence.

Fig. 3 shows the average BER versus jitter standard deviation when various values of correlation coefficient are assumed. The mixed PRS-based RF-FSO system with $M = 4$ relays is considered. Two scenarios are analyzed: the relay

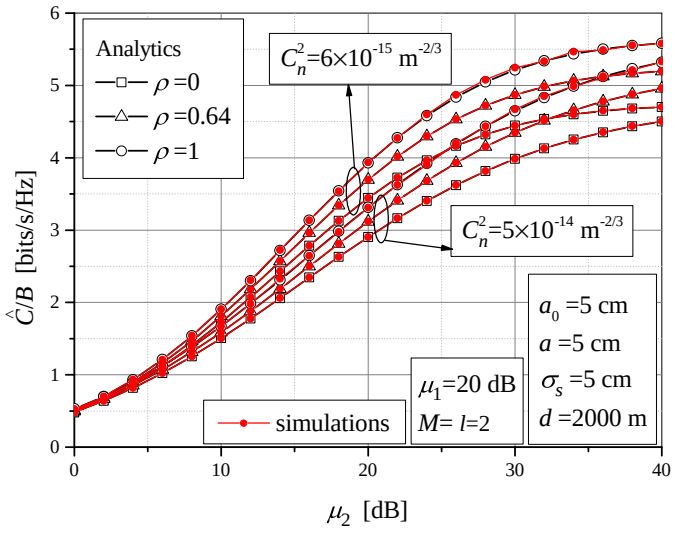

Figure 6: Ergodic capacity vs. μ_2 in various atmospheric turbulence conditions for different values of correlation coefficient

with best estimated CSI can perform further transmission ($l = M = 4$); and all relays except the one with worst estimated CSI are unavailable ($l = 1$). Greater value of correlation coefficient (meaning the outdated CSI, which is employed for determining of the relay amplification, and the actual CSI at the time of transmission are more dependent and correlated) leads to better system performance when the best relay transmits the signal. On the other hand, when only the worst one is ready for transmission, greater value of correlation coefficient degrades the system performance. With lowering the correlation coefficient ($\rho \to 0$), outdated and actual CSIs are more independent. In this scenario, it can be decided with high probability that the active relay is not the worst one among all relays, leading to the better system performance. When outdated and actual CSIs are completely uncorrelated, the system performance for the case of $l = 1$ and $l = M$ are the same. This occurs since the CSIs are independent and the relay selection has no impact on the system performance.

Furthermore, Fig. 3 shows that the pointing errors have strong effect on BER performance, especially when the correlation coefficient is greater. Also,

the effect of correlation on the average BER is more pronounced when the value of jitter standard deviation is smaller (corresponding to the weaker pointing errors). In the case of very high values of σ_s ($\sigma_s > 0.4$), the correlation impact on the RF-FSO system performance is poor and can be neglected.

Fig. 4 presents the average BER in the function of $\mu_1 = \mu_2$, considering weak and strong atmospheric turbulence and the correlation coefficient $\rho = 0$, $\rho = 0.72$, and $\rho = 1$. It can be observed that greater values of ρ bring about the improved average BER performance, especially in weak atmospheric turbulence. When second FSO link is affected by convenient conditions (weak atmospheric turbulence), the effect of correlation on the average BER is strong. In the case the transmission of the optical signal is affected by strong and harmful atmospheric turbulence, the influence of correlation is less significant.

The ergodic capacity versus jitter standard deviation, when various values of correlation coefficient are assumed, is shown in Fig. 5. The cases wherein the selected relay is with the best and the worst estimated CSIs, are observed. The same effect as in Fig. 3 is noticed: the increase of ρ improves ergodic capacity performance when $l = M$, while performance degradation is noticed when $l = 1$. Also, the capacity performance when $\rho = 0$ is the same for both cases. Contrary to the average BER, it is interesting to note that the pointing errors (determined by σ_s) do not play a major role in the ergodic capacity performance. In addition, the intensity of correlation impact on the ergodic capacity is independent of the pointing errors strength.

The ergodic capacity versus the electrical SNR per FSO hop, when the optical signal transmission is performed via channel influenced by various atmospheric turbulence conditions, is presented in Fig. 6. Equivalent to Fig. 4, the capacity performance is better when the FSO link is affected by weak atmospheric turbulence, and when the coefficient correlation is greater. Also, the correlation impact on the ergodic capacity is less dependent on the atmospheric turbulence compared to the average BER performance (see Fig. 4).

The ergodic capacity dependence on the electrical SNR over FSO hop is depicted in Fig. 7, considering different values of the parameter ρ. The average

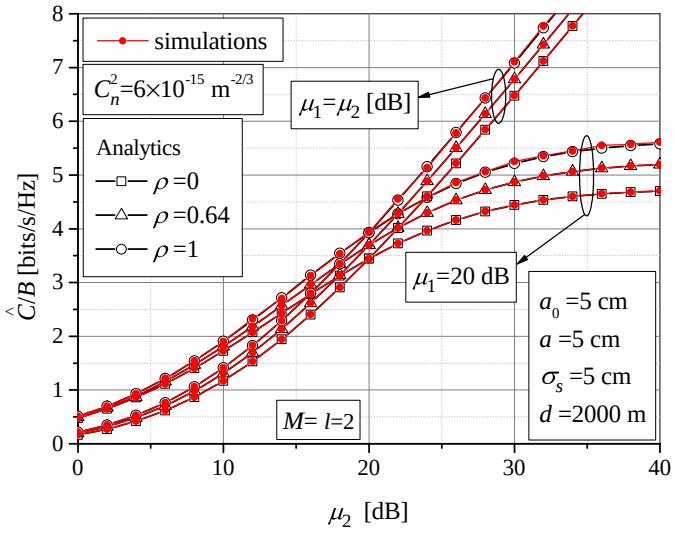

Figure 7: Ergodic capacity vs. μ_2 in various atmospheric turbulence conditions for different values of correlation coefficient

SNR per RF link is $\mu_1 = 20$ dB or $\mu_1 = \mu_2$. The ergodic capacity performance is improved with greater values of ρ. Similar to Fig. 2, the ergodic capacity floor exists when μ_1 is constant, so the system performance betterment will not be achieved by further increase in the signal power. The capacity floor occurs in the range of lower values of μ_2 when ρ is lower. Contrary, when the average SNR over RF hop increases simultaneously with the electrical SNR over FSO hop, the ergodic capacity floor does not appear.

The ergodic capacity versus the number of relays for various size of normalized jitter standard deviations is shown in Fig. 8. It is considered that the range of the FSO hop is $d = 2000$ m and $d = 6000$ m. The ergodic capacity performance is better when the FSO link length is shorter, as well as when σ_s/a is lower, which corresponds to weaker effect of the misalignment fading. Furthermore, the effect of pointing errors is more dominant when the propagation distance from relay to destination is shorter thereby implying favorable FSO channel conditions.

The ergodic capacity dependence on the number of relays for different values

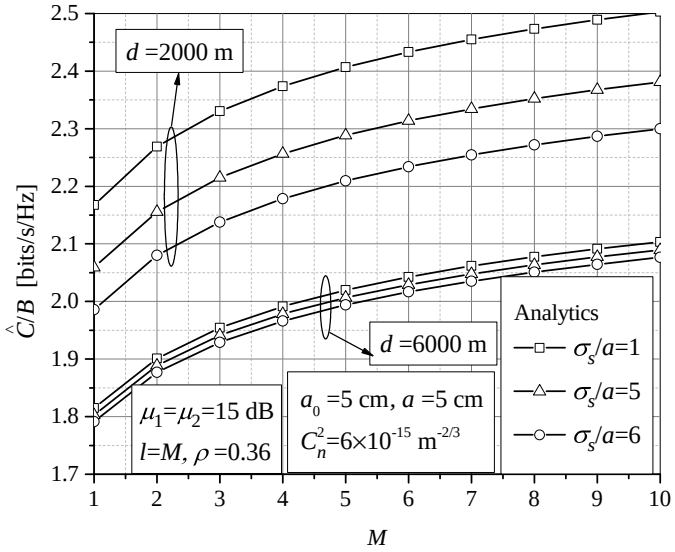

Figure 8: Ergodic capacity vs. the number of relays for different values of FSO link length

of the parameters ρ and σ_s/a is shown in Fig. 9. When $\rho = 0$, the outdated and actual CSIs are totally uncorrelated, and the relay selection has no influence on the ergodic capacity performance. For that reason, the constant value of the capacity is obtained when $\rho = 0$. Furthermore, it is observed that the effect of correlation on the ergodic capacity is almost independent on the pointing errors strength. Also, the greatest SNR gain is achieved by employing the PRS system with two relays compared with the one with only one relay.

The ergodic capacity versus correlation coefficient is presented in Fig. 10, considering weak, moderate and strong atmospheric turbulence conditions. As it has been concluded, greater values of ρ lead to improved ergodic capacity performance. In other words, when outdated CSI employed for the relay amplification adjustment and the actual CSI at the time of transmission are more correlated, the value of ergodic capacity is greater. In addition, the slope of capacity curves vs. ρ are the same for all atmospheric turbulence conditions.

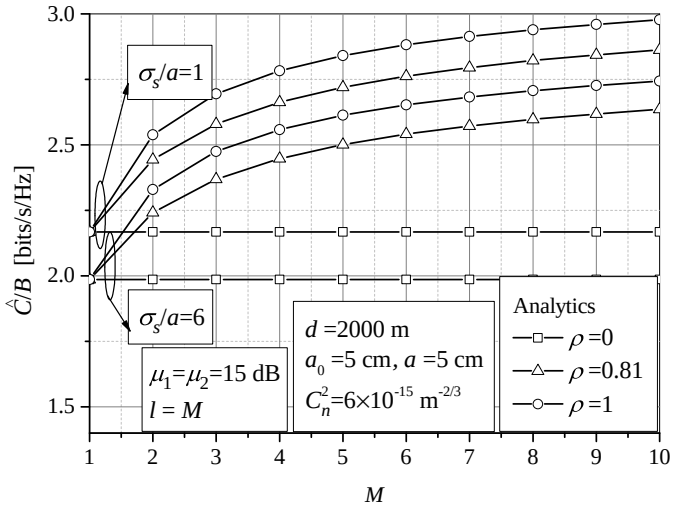

Figure 9: Ergodic capacity vs. the number of relays for different values of correlation coefficient

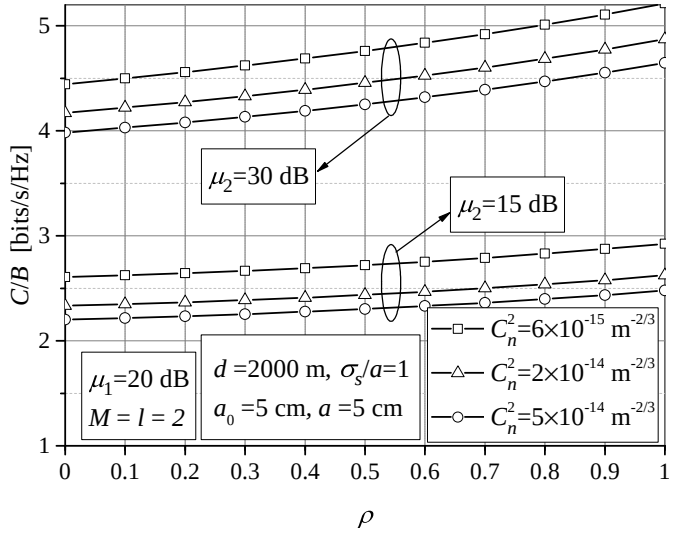

Figure 10: Ergodic capacity vs. correlation coefficient

5. Concluding remarks

We have analyzed the average BER and the ergodic capacity dependence on atmospheric turbulence, pointing errors strength, correlation coefficient, electrical SNR per FSO hop, average SNR per RF hop, and different PRS structures.

It has been concluded that the temporal correlation coefficient is an important parameter influencing the system performance. Greater values of the correlation coefficient (i.e., meaning that the outdated CSI and actual CSI of the source-relay channel at the time of signal transmission are more correlated) lead to improvement of the average BER (ergodic capaciy) performance in the case when the relay with best estimated CSI is available. Contrary, average BER (ergodic capacity) performance becomes worse with increasing correlation coefficient in the case when all relays except the one with the worst estimated CSI are unavailable. When the correlation coefficient is equal to zero, the average BER (ergodic capacity) performance is the same independently if the best or the worst relay is selected.

Furthermore, the impact of correlation on the average BER is more pronounced in the case when the FSO signal experiences friendly environment with favorable conditions (weak pointing errors and weak atmospheric turbulence). On the other hand, the slope of the ergodic capacity curve vs. correlation coefficient is approximately the same in all turbulence conditions of FSO link. In addition, the following conclusion follows: the larger the value of correlation coefficient, the stronger is the effect of number of relays on the ergodic capacity.

Acknowledgment

The work of M. I. Petkovic has received funding from the European Union Horizon 2020 research and innovation programme under the Marie Skodowska-Curie grant agreement No 734331. This work was partially supported by the Ministry of Education, Science and Technology Development of the Republic of Serbia under Grants TR-32035, TR-32028 and III-44006, as well as COST Action CA16220.

References

[1] O. Tipmongkolsilp, S. Zaghloul, and A. Jukan,, "The evolution of cellular backhaul technologies: Current issues and future trends, " *IEEE Communi-*

cations Surveys & Tutorials, vol. 13, no. 1, pp. 97–113, 2011.

[2] P. V. Trinh, T. Cong Thang, and A. T. Pham, "Mixed mmWave RF/FSO relaying systems over generalized fading channels with pointing errors," *IEEE Photonics Journal*, vol. 9, no. 1, pp. 1–14, Feb. 2017.

[3] A. T. Pham, P. V. Trinh, V. V. Mai, N. T. Dang, and Cong-Thang Truong, "Hybrid free-space optics/millimeter-wave architecture for 5G cellular backhaul networks," in *Proc. 2015 Opto-Electronics and Communications Conference (OECC)*, Shanghai, 2015, pp. 1–3.

[4] J. A. Mendenhall, et. al., "Design of an optical photon counting array receiver system for deep space communications," In. *Proc. of the IEEE*, Oct. 2007.

[5] D. O. Caplan, et al., "Ultra-wide-range multi-rate DPSK laser communications," In. *Proc. CLEO/QELS: 2010 Laser Science to Photonic Applications*, San Jose, CA, 2010, pp. 1–2.

[6] N. W. Spellmeyer, et al., "Demonstration of multi-rate thresholded preamplified 16-ary pulse-position-modulation," *Proc. 2010 Conference on Optical Fiber Communication (OFC/NFOEC), collocated National Fiber Optic Engineers Conference*, San Diego, CA, 2010, pp. 1–3.

[7] N. W. Spellmeyer, et al., "A multi-rate modem for free-space laser communications," in *Proc. SPIE 8971,* 2014.

[8] D. M. Boroson and B. S. Robinson "The lunar laser communication demonstration: NASA's first step toward very high data rate support of science and exploration missions," *Space Sci. Reviews Journal,* vol. 185, no. 14, pp 115-1282014.

[9] E. Ciaramella, Y. Arimoto, G. Constabile, M. Presi, A. DErrico, and M. Matsumoto, "1.28 Terabit/s (32X40 Gbit/s) WDM transmission system for free space optical communications," IEEE Journal on Selected Areas in Communications, vol. 27, no. 9, pp. 1639–1645, Dec. 2009.

[10] D. Messier, DLR Researchers Set World Record in Free-space Optical Communications, Available on: http://www.parabolicarc.com/2016/11/05/dlr-researchers-set-world-record-freespace-optical-communications/

[11] Z. Ghassemlooy, W. Popoola, and S. Rajbhandari, *Optical Wireless Communications: System and Channel Modelling with MATLAB*. Boca Raton, USA: CRC Press, 2013.

[12] H. Kaushal, V. K. Jain, S. Kar, *Free Space Optical Communication*. New Delhi, India: Springer, 2017.

[13] A. A. Farid and S. Hranilovic, "Outage capacity optimization for free space optical links with pointing errors," *IEEE/OSA Journal of Lightwave Technology*, vol. 25, no. 7, pp. 1702–1710, Jul. 2007.

[14] H. G. Sandalidis, T. A. Tsiftsis, and G. K. Karagiannidis, "Optical wireless communications with heterodyne detection over turbulence channels with pointing errors," *IEEE/OSA Journal of Lightwave Technology*, vol. 27, no. 20, pp. 4440 – 4445, Oct. 2009.

[15] H. G. Sandalidis, "Optimization models for misalignment fading mitigation in optical wireless links," *IEEE Communication Letters*, vol. 12, no. 5, pp. 395–397, May 2008.

[16] A. A. Farid and S. Hranilovic, "Outage capacity for MISO intensity-modulated free-space optical links with misalignment," *IEEE/OSA Journal of Optical Communications and Networking*, vol. 3, no. 10, pp. 780–789, Oct. 2011.

[17] L. C. Andrews and R. N. Philips, *Laser Beam Propagation through Random Media*. 2nd ed., Bellingham, Washington, USA: Spie Press, 2005.

[18] M. A. Al–Habash, L. C. Andrews, and R. N. Philips, "Mathematical model for the irradiance probability density function of a laser beam propagating through turbulent media," *Optical Engineering*, vol. 40, no. 8, pp. 1554–1562, Aug. 2001.

[19] M. A. Khalighi and M. Uysal, "Survey on free space optical communication: A communication theory perspective," *IEEE Communications Surveys & Tutorials*, vol. 16, no. 4, pp.2231–2258, Fourthquarter 2014.

[20] N. D. Chatzidiamantis and G. K. Karagiannidis, "On the distribution of the sum of Gamma-Gamma variates and applications in RF and optical wireless communications," *IEEE Transactions on Communications*, vol. 59, no. 5, pp. 1298–1308, May 2011.

[21] E. Lee, J. Park, D. Han, and G. Yoon, "Performance analysis of the asymmetric dual-hop relay transmission with mixed RF/FSO links," *IEEE Photonic Technology Letters*, vol. 23, no. 21, pp. 1642–1644, Nov. 2011.

[22] H. Samimi and M. Uysal, "End-to-end performance of mixed RF/FSO transmission systems," *IEEE/OSA Journal of Optical Communications and Networking*, vol. 5, no. 11, pp. 1139–1144, Nov. 2013.

[23] I. S. Ansari, F. Yilmaz, and M.−S. Alouini, "Impact of pointing errors on the performance of mixed RF/FSO dual-hop transmission systems," *IEEE Wireless Communications Letters*, vol. 2, no. 3, pp. 351–354, Jun. 2013.

[24] I. S. Ansari, F. Yilmaz, and M.−S. Alouini, "On the performance of mixed RF/FSO dual-hop transmission systems," in *Proc. 2013 IEEE 77th Vehicular Technology Conference (VTC Spring)*, Jun. 2013, pp. 1–5.

[25] I. S. Ansari, F. Yilmaz, and M.−S. Alouini, "On the performance of hybrid RF and RF/FSO fixed gain dual-hop transmission systems," in *Proc. 2013 Saudi International Electronics, Communications and Photonics Conference (SIECPC)*, Apr. 2013, pp. 1–6.

[26] S. Anees and M. R. Bhatnagar, "Performance analysis of amplify-and-forward dual-hop mixed RF/FSO systems," in *Proc. 2014 IEEE 80th Vehicular Technology Conference (VTC Fall)*, Vancouver, BC, Apr. 2014.

[27] S. Anees and M. R. Bhatnagar, "Performance of an amplify-and-forward dual-hop asymmetric RF/FSO communication system," *IEEE/OSA Journal*

of Optical Communications and Networking, vol. 7, no. 2, pp. 124–135, Jun. 2015.

[28] Z. Jiayi, D. Linglong, Z. Yu, and W. Zhaocheng, "Unified performance analysis of mixed radio frequency/free-space optical dual hop transmission systems," *Journal of Lightwave Technology*, vol. 33, no. 11, pp. 2286–2293, Jun. 2015.

[29] E. Zedini, I. S. Ansari, and M.–S. Alouini, "Unified performance analysis of mixed line of sight RF-FSO fixed gain dual-hop transmission systems," in *Proc. 2015 IEEE Wireless Communications and Networking Conference (WCNC)*, New Orleans, LA, Mar. 2015, pp. 46–51.

[30] E. Soleimani-Nasab and M. Uysal, "Generalized performance analysis of mixed RF/FSO systems," in *Proc. 2014 3rd International Workshop in Optical Wireless Communications (IWOW)*, Funchal, 2014, pp. 16–20.

[31] E. Zedini, I. S. Ansari, and M.–S. Alouini, "Performance analysis of mixed Nakagami-m and Gamma-Gamma dual-hop FSO transmission systems," *IEEE Photonics Journal*, vol. 7, no. 1, pp. 1–20, Feb. 2015.

[32] Y. Liang, M. O. Hasna, and X. Gao, "Performance of mixed RF/FSO with variable gain over generalized atmospheric turbulence channels," *IEEE Journal on Selected Areas in Communications*, vol. 33, no. 9, pp. 1913–1924, Sep. 2015.

[33] G. T. Djordjevic, M. I. Petkovic, A. M. Cvetkovic, and G. K. Karagiannidis, "Mixed RF/FSO relaying with outdated channel state information," *IEEE Journal on Selected Areas in Communications*, vol. 33, no. 9, pp. 1935–1948, Sep. 2015.

[34] I. S. Ansari, F. Yilmaz, and M.−S. Alouini, "On the performance of mixed RF/FSO variable gain dual-hop transmission systems with pointing errors," in *Proc. 2013 IEEE 78th Vehicular Technology Conference (VTC Fall)*, Sep. 2013, pp. 1−5.

[35] I. S. Ansari, F. Yilmaz, and M.−S. Alouini, "On the performance of hybrid RF and RF/FSO dual-hop transmission systems," *2nd International Workshop on Optical Wireless Communications (IWOW 2013)*, Newcastle Upon Tyne, UK, Oct. 2013, pp. 45−49.

[36] S. Anees, P. Meerur and M. R. Bhatnagar, "Performance analysis of a DF based dual hop mixed RF-FSO system with a direct RF link," in Proc. *2015 IEEE Global Conference on Signal and Information Processing (GlobalSIP)*, Orlando, FL, 2015, pp. 1332–1336.

[37] E. Soleimani-Nasab and M. Uysal, "Generalized performance analysis of mixed RF/FSO cooperative systems," *IEEE Transactions on Wireless Communications*, vol. 15, no. 1, pp. 714–727, Jan. 2016.

[38] M. I. Petkovic, A. M. Cvetkovic, G. T. Djordjevic, andG. K. Karagiannidis, "Outage performance of the mixed RF/FSO relaying channel in the presence of interference," *Wireless Personal Communications*, vol. 96, no. 2, pp. 2999–3014, Sept. 2017.

[39] V. Jamali, D. S. Michalopoulos, M. Uysal, and R. Schober, "Link allocation for multiuser systems with hybrid RF/FSO backhaul: Delay-limited and delay-tolerant designs," *IEEE Transactions on Wireless Communications*, vol. 15, no. 5, pp. 3281–3295, May 2016.

[40] J. Feng and X. Zhao, "Performance analysis of mixed RF/FSO systems with STBC users", *Optics Communications*, vol. 381, pp. 244–252, Dec. 2016.

[41] I. A. Alimi, P. P. Monteiro, and A. L. Teixeira, "Analysis of multiuser mixed RF/FSO relay networks for performance improvements in Cloud Computing-Based Radio Access Networks (CC-RANs)", *Optics Communications*, vol. 402, pp. 653–661, Nov. 2017.

[42] L. Yang, M. O. Hasna, and I. S. Ansari, "Unified performance analysis for multiuser mixed η - μ and $\mathcal{M}$ - distribution dual-hop RF/FSO systems,"

IEEE Transactions on Communications, vol. 65, no. 8, pp. 3601–3613, Aug. 2017.

[43] S. Anees, P. S. S. Harsha and M. R. Bhatnagar, "On the performance of AF based mixed triple-hop RF/FSO/RF communication system," in P*roc. 2017 IEEE 28th Annual International Symposium on Personal, Indoor, and Mobile Radio Communications (PIMRC)*, Montreal, QC, 2017, pp. 1–6.

[44] S. Anees, M. R. Bhatnagar and P. Ram, "On the performance of DF based mixed triple-hop RF-FSO-RF cooperative system," in *Proc. 2017 International Conference on Recent Innovations in Signal processing and Embedded Systems (RISE)*, Bhopal, 2017, pp. 55–61.

[45] N. D. Chatzidiamantis, D. S. Michalopoulos, E. E. Kriezis, G. K. Karagiannidis, and R. Schober, "Relay selection protocols for relay-assisted free-space optical systems," *IEEE/OSA Journal of Optical Communications and Networking*, vol. 5, no. 1, pp. 92-103, Jan. 2013.

[46] N. D. Chatzidiamantis, D. S. Michalopoulos, E. E. Kriezis, G. K. Karagiannidis, and R. Schober, "Relay selection in relay-assisted free space optical systems," in *Proc. 2011 IEEE Global Telecommunications Conference (GLOBECOM)*, Dec. 2011, pp. 1–6.

[47] I. Krikidis, J. Thompson, S. Mclaughlin, and N. Goertz, "Amplify-and-forward with partial relay selection," *IEEE Communication Letters*, vol. 12, no. 4, pp. 235-237, Apr. 2008.

[48] D. B. Da Costa and S.Aïssa, "End-to-end performance of dual-hop semi-blind relaying systems with partial relay selection," *IEEE Transactions on Wireless Communications*, vol. 8, no. 8, pp. 4306-4315, Aug. 2009.

[49] H. A. Suraweera, D. S. Michalopoulos, and G. K. Karagiannidis, "Semi-blind amplify-and-forward with partial relay selection," *Electronics Letters*, vol. 45, no. 6, pp. 317–319, Mar. 2009.

[50] H. A. Suraweera, M. Soysa, C. Tellambura, and H. K. Garg, "Performance analysis of partial relay selection with feedback delay," *IEEE Signal Processing Letters*, vol. 17, no. 6, pp. 531–534, Jun. 2010.

[51] M. Soysa, H. A. Suraweera, C. Tellambura, and H. K. Garg, "Partial and opportunistic relay selection with outdated channel estimates," *IEEE Transactions on Communications*, vol. 60, no. 3, pp. 840–850, Mar. 2012.

[52] D. S. Michalopoulos, H. A. Suraweera, G. K. Karagiannidis, and R. Schober, "Amplify-and-forward relay selection with outdated channel estimates," *IEEE Transactions on Communications*, vol. 60, no. 5, pp. 1278–1290, May 2012.

[53] M. I. Petkovic, A. M. Cvetkovic, G. T. Djordjevic, and G. K. Karagiannidis, "Partial relay selection with outdated channel state estimation in mixed RF/FSO systems," *IEEE Journal of Lightwave Technology*, vol. 33, no. 13, pp. 2860–2867, Jul. 2015.

[54] M. I. Petkovic, A. M. Cvetkovic, and G. T. Djordjevic, "Mixed RF/FSO relaying systems," in *Optical Wireless Communications – An Emerging Technology*, Springer, 2016.

[55] G. N. Kamga and S. Aissa, "Relay selection based hybrid RF/FSO transmission over Double Generalized Gamma channels under outdated CSI and pointing errors," in *Proc. 2018 IEEE International Conference on Communications (ICC)*, Kansas City, MO, 2018, pp. 1–6.

[56] E. Balti, M. Guizani, B. Hamdaoui, and Y. Maalej, "Partial relay selection for hybrid RF/FSO systems with hardware impairments," in *Proc. 2016 IEEE Global Communications Conference (GLOBECOM)*, Washington, DC, 2016, pp. 1–6.

[57] E. Balti, M. Guizani, B. Hamdaoui and B. Khalfi, "Aggregate hardware impairments over mixed RF/FSO relaying systems with outdated CSI," *IEEE Transactions on Communications*, vol. 66, no. 3, pp. 1110–1123, March 2018.

[58] I. S. Gradshteyn and I. M. Ryzhik, *Table of Integrals, Series, and Products.* 6th ed., New York: Academic, 2000.

[59] E. J. Lee, V. W. S. Chan, "Part 1: optical communication over the clear turbulent atmospheric channel using diversity," *IEEE Journal on Selected Areas in Communications,* vol. 22, no. 9, pp. 1896-1906, Nov. 2004.

[60] T. S. Rappaport, *Wireless communications: principles and practice.* vol. 2. New Jersey: prentice hall PTR, 1996.

[61] The Wolfarm Functions Site, 2008. [Online] Available: http:/functions.wolfarm.com.

[62] M. K. Simon and M.−S. Alouni, *Digital Communication over Fading Channels.* 2nd ed., New York, NY: John Wiley & Sons Inc., 2004.

[63] I. S. Ansari, S. Al−Ahmadi, F. Yilmaz, M.−S. Alouini, and H. Yanikomeroglu, "A new formula for the BER of binary modulations with dual-branch selection over generalized-K composite fading channels," *IEEE Transactions on Communications*, vol. 59, no. 10, pp. 2654−2658, Oct. 2011.

[64] I. S. Ansari, F. Yilmaz, and M.–S. Alouini, "Performance analysis of free-space optical links over Málaga ($\mathcal{M}$) turbulence channels with pointing errors," *IEEE Transactions on Wireless Communications*, vol. 15, no. 1, pp. 91-102, Jan. 2016.

[65] I. S. Ansari, M.–S. Alouini, and J. Cheng, "Ergodic capacity analysis of free-space optical links with nonzero boresight pointing errors," *IEEE Transactions on Wireless Communications*, vol. 14, pp. 4248–4264, Aug. 2015.

[66] A. Annamalai, R. C. Palatu, and J. Matyjas, "Estimating ergodic capacity of cooperative analog relaying under different adaptive source transmission techniques," in *Proc. 2010 IEEE Sarnoff Symposium*, Apr. 2010, pp. 1–5.

[67] S. C. Gupta, "Integrals involving products of G-functions," *Proc. of the National Academy of Sciences, India*, vol. 39(A), no. II, 1969.